Title: Room Temperature Phosphorescence based Dissolved Oxygen Detection by Core-shell Polymer Nanoparticles having Metal-free Organic Phosphor

Authors: Jinsang Kim, Ph.D.; Youngchang Yu; Min Sang Kwon; Jaehun Jung; Mounggon Kim; Kyeongwoon Chung; Johannes Gierschner; Ji Ho Youk; Sergey Borisov; Yingying Zeng

To be cited as: 10.1002/anie.201708606

Link to VoR: https://doi.org/10.1002/anie.201708606

Room Temperature Phosphorescence based Dissolved Oxygen Detection by Core-shell Polymer Nanoparticles having Metal-free Organic Phosphor

Youngchang Yu,[†] Min Sang Kwon,[†,*] Jaehun Jung, Yingying Zeng, Mounggon Kim, Kyeongwoon Chung, Johannes Gierschner, Ji Ho Youk,* Sergey M. Borisov,* and Jinsang Kim*

Dedication ((optional))

Abstract: Highly sensitive optical detection of oxygen including dissolved oxygen (DO) is of great interest in various applications. We devised a novel room temperature phosphorescence (RTP) based oxygen detection platform by constructing core-shell nanoparticles with water-soluble polymethyloxazoline shells and oxygen-permeable polystyrene core crosslinked with metal-free purely organic phosphors. The resulting nanoparticles show a very high sensitivity (limit of detection (LOD) of 60nM DO) and can be readily used for oxygen quantification in aqueous environments as well as gaseous phase.

Quantification of dissolved oxygen (DO) in concentration ranges of 1μM and below has recently attracted considerable attention for its urgent needs in numerous applications such as corrosion protection,[1] surface treatment,[2] semiconductor industry,[3] and biological research.[4] Although few detection systems such as membrane inlet mass spectrometry (MIMS) and purge-and-trap gas chromatography-mass spectrometry (P&T) are able to quantify at a low level, complex, bulky and expensive equipment is not portable and requires trained personnel for operation, limiting its applicability for convenient and easy monitoring of DO.[4]

Optical sensors have recently become a crucial tool for quantification of DO due to their advantageous characteristics such as minimal invasiveness, miniaturization capability, versatility in formats, and suitable 2D or 3D imaging of DO distribution.[5,6] Optical detection of DO mostly relies on the phosphorescent transition metal complexes such as polypyridyl complexes of ruthenium(II) and Pd(II) and Pt(II) porphyrins because they possess significantly long decay lifetimes which ensure efficient energy transfer to molecular oxygen, resulting in complete quenching of phosphorescence emission at very low DO concentration.[6] However, concerns about the high cost, unclear toxicities, and sustainability of precious metals have incited the research community to investigate novel optical DO indicators from more abundant materials.

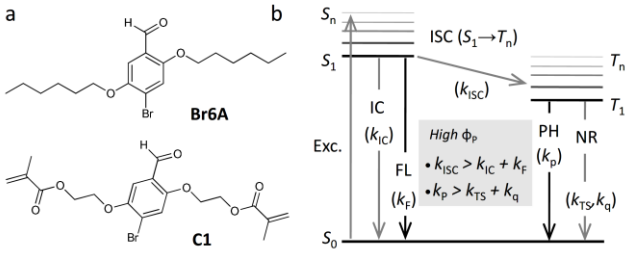

Figure 1. (a) Chemical structures of the designed crosslinkable phosphor, C1 and a control, Br6A, are shown. (b) A common Jablonski diagram of organic emitters

Metal-free organic phosphors are an emerging alternative of organometallic phosphors in a wide range of applications including organic light emitting diodes (OLEDs), bio-imaging and sensors.[7] This new class of organic emitters can be particularly useful for highly sensitive optical DO detection due to a) a long decay time (from millisecond to second) originated from their inefficient spin-orbit coupling (SOC) and b) large Stokes shifts,[8] which enables spectral separation of excitation and emission wavelength resulting in simple optical set-up and low-interference measurements. However, despite vast potential, metal-free organic phosphors have largely unexplored as DO indicators.[9,10,11b]

Although substantial progress has been made in the field of metal-free organic phosphors since the pioneer works from the groups of Fraser,[11] Kim,[12] and Tang,[13] bright organic phosphors at room temperature are still very rare and only limited to BF_2-chelates,[9,11,14] phenylthiobenzene,[15] benzophenone,[13,16,17] fluorene,[18,19] triazine,[20] boronic ester,[21] naphthalimide,[22] sulfone,[23] bromobenzaldehyde,[12] *and polyaromatic* analogues.[24,25] In addition, stringent conditions of rigid hosts such as crystalline solid-state structures and carefully chosen polymer matrices are commonly required for bright room temperature phosphorescence (RTP). However, practical applicability of such a phosphors-doped polymer film and a

[a] Y. Yu,[1,†] M. S. Kwon,[1,†,*] J. Jung,[2] Y, Zeng,[1] M. Kim,[1] K. Chung,[2] J. Kim[1,2,3,4,5,*]
[1]Department of Materials Science and Engineering, [2]Macromolecular Science and Engineering, [3]Department of Chemical Engineering, [4]Department of Biomedical Engineering, [5]Department of Chemistry, University of Michigan
E-mail: jinsang@umich.edu
[b] M. S. Kwon[6,*]
[6]Department of Materials Science and Engineering
Ulsan Institute of Science and Technology (UNIST)
E-mail: kwonms@unist.ac.kr
[c] K. Chung[7]
[7]Process Innovation Department
Korea Institute of Materials Science (KIMS)
[d] J. Gierschner[8]
[8]Madrid Institute for Advanced Studies – IMEDA Nanoscience
[e] J. Youk[9,*]
[9]Department of Applied Organic Materials Engineering
Inha University
E-mail: youk@inha.ac.kr
[f] S. Borisov[10,*]
[10]Institue of Analytical Chemistry and Food Chemistry
Graz University of Technology
E-mail: sergey.borisov@tugraz.at
[†] These authors contributed equally to this work.

Supporting information for this article is given via a link at the end of the document.

phosphorescent crystal can be rather limited and hence, development of a new versatile platform that allows to achieve bright organic RTP and thus to quantify DO at significantly low concentration for various applications is required.

Here, we report metal-free organic phosphors crosslinked within core-shell polymer nanoparticles as a novel versatile platform for highly sensitive detection of DO as nanoparticles have proven to be a versatile platform for various applications including DO quantification.[26] To achieve high sensitivity, for the core part of the nanoparticles we chose metal-free organic phosphors as an indicator considering their long phosphorescence decay time and polystyrene (PS) as a matrix due to its high oxygen permeability. Poly(2-methyl-2-oxazoline) (PMeOx) was selected as an outer shell of the nanoparticles because of its water solubility and biocompatibility, enabling the application of DO quantification in aqueous phase for a variety of applications. Most importantly, a novel metal-free organic phosphor was rationally designed to be used as a cross-linker as well as an indicator since the restriction of molecular motions near the phosphors by covalent crosslinking through a short linker will greatly enhance phosphorescence intensity, allowing for highly sensitive detection of DO (see Figure 1). Phosphorescent core-shell nanoparticles having a well-defined diameter of ca. 180 nm and 320 nm were successfully prepared by reversible addition-fragmentation chain-transfer (RAFT) dispersion polymerization of a macro-RAFT agent in the presence of the newly designed metal-free organic phosphor having a cross-linking capability (see Figure 2 and SI).[12d]

The realization of bright RTP from metal-free organic phosphors in non-rigid matrix such as a polymeric nanoparticle is still a challenging issue; as far as we know, only a few examples have been reported until now.[11] Active molecular motions in non-rigid matrix greatly promotes the radiationless decay processes such as triplet-triplet energy transfer and intersystem crossing (ISC) from T_1 to S_0, resulting in complete quenching of phosphorescence (see Figure 1b).[12,19] In fact, simple doping of a metal-free organic phosphor, Br6A, into polymeric nanoparticles showed weak phosphorescence emission even under inert atmosphere. To address the challenge, we introduce cross-links between phosphors and polymers into the nanoparticle system.

The phosphor with a short saturated hydrocarbon linker (denoted as C1) was designed and synthesized as the DO indicator (see Figure 1a). To validate our molecular design, we prepared a poly(methyl methacrylate) (PMMA) having covalently crosslinked C1 and compared its phosphorescence quantum efficiency with a Br6A doped PMMA film (see the SI). As expected, C1-crosslinked PMMA showed high phosphorescence quantum efficiency of ca. 40%, which is ca. 3 times higher compared to the Br6A doped film. This is attributed to the fact that a short and simple cross-linker efficiently restricts the molecular motions of phosphors as well as the polymer matrix, and thereby effectively suppresses the nonradiative relaxation pathways.[12d]

We then prepared crosslinked core-shell polymeric nanoparticles based on the C1 phosphors. A macro-RAFT initiator was synthesized via a tosyl-functionalized RAFT agent as a dual initiator in two steps.[27] Water-soluble PMeOx was first synthesized by ring opening polymerization (ROP) of methyloxazoline (MeOx) at 80 °C followed by the RAFT polymerization of acrylamide (AAm) in the presence of AIBN (see Figure 2, step 1). Importantly, a PAAm block was introduced to promote the rate of RAFT polymerization of styrene[28] since the RAFT initiator is not effective for polymerization of styrene monomers (see Figure 2, step 2).[29] Once the macro-RAFT initiator was successfully prepared, the core-shell nanoparticles were then prepared through an one-pot dispersion RAFT polymerization of styrene monomers together with C1 by means of the macro-RAFT agent (see Figure 2, step 3). The resulting crosslinked amphiphilic block copolymers spontaneously self-assembled into well-defined functional core-shell nanoparticles (see Figure 2, step 4). The size of nanoparticle could be manipulated by controlling the amount of the macroinitiator (see the SI).

The resulting core-shell nanoparticles were characterized by scanning electron microscope (SEM), dynamic light scattering (DLS) and by emission and excitation photoluminescence (PL) spectroscopy. SEM and DLS analyses confirmed the formation of the core-shell nanoparticles with average diameters of ca. 180 nm and ca. 320 nm, respectively, and a narrow size distribution (see Figure S1 and S2). Figure 3a shows the PL excitation spectrum of C1-crosslinked nanoparticles which matches well with the absorption spectrum of Br6A, clearly indicating that C1 was successfully incorporated into the nanoparticles (see Figure S3). As expected, the nanoparticles exhibited a distinct oxygen sensitivity. While the nanoparticles show essentially no phosphorescent at ambient conditions, bright phosphorescence was observed after the elimination of oxygen by nitrogen purging (see Figure 3a, inset).

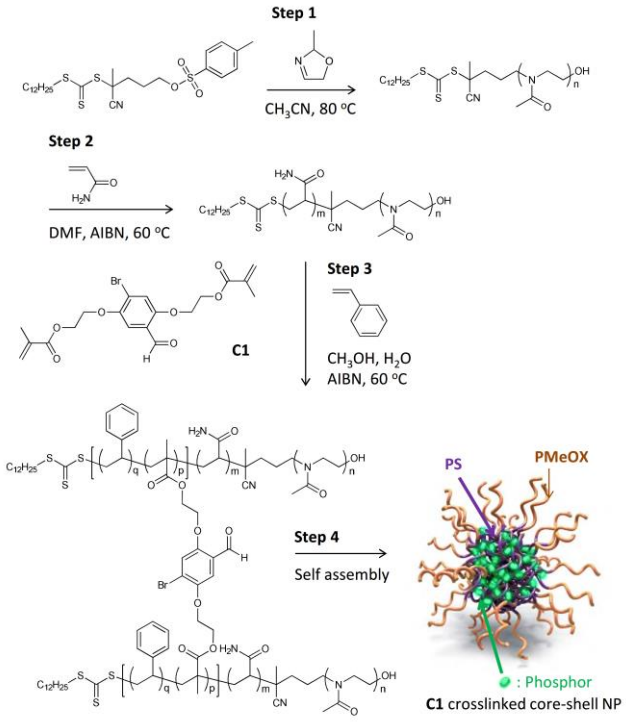

Figure 2. Synthetic routes of C1-crosslinked NPs are presented.

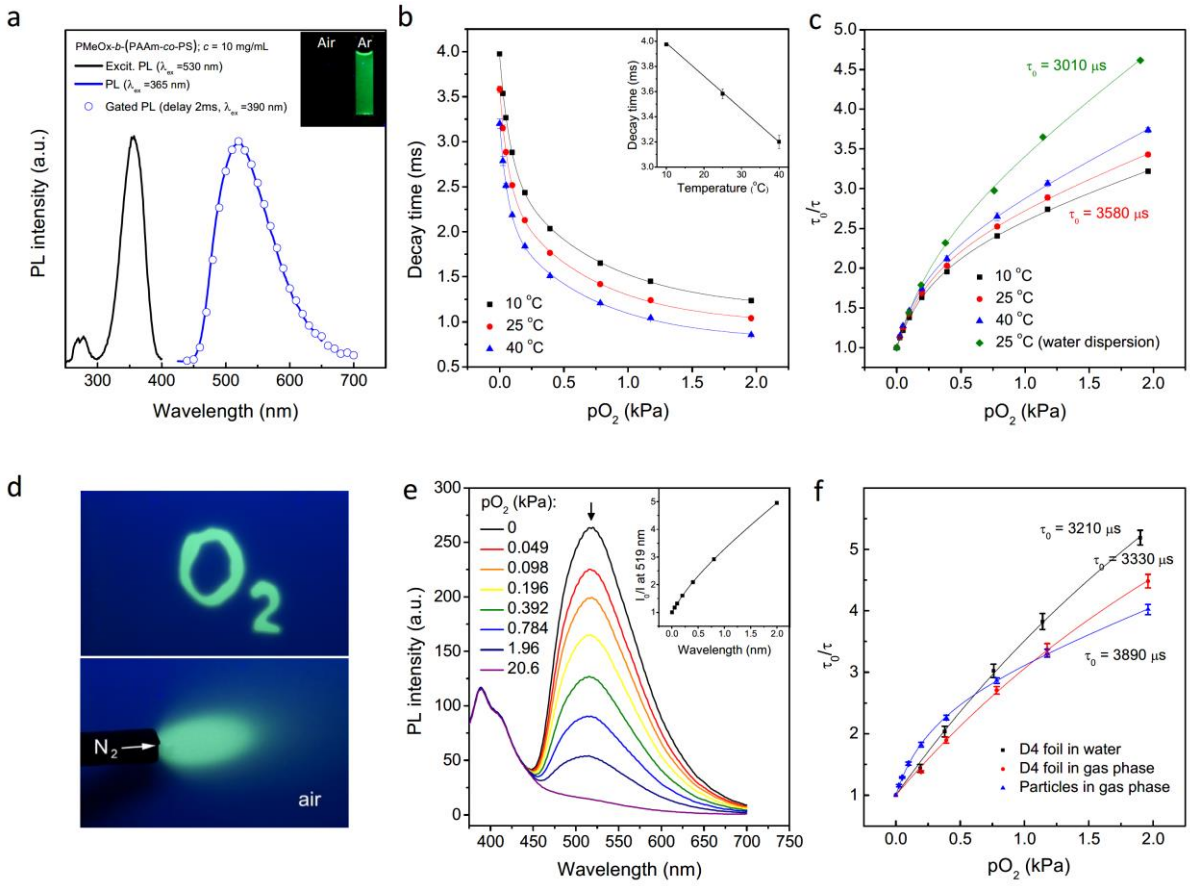

Figure 3. (a) Photoluminescence (PL) emission and excitation, and gated PL spectra of phosphors cross-linked NPs dispersed in argon saturated water. The inset shows PL images of phosphors cross-linked NPs dispersed in air-saturated (left) and argon-saturated (right) water at room temperature under a 365 nm hand held UV light. (b) Decay time plots and temperature dependency of τ_0 (inset) and (c) Stern-Volmer plots of dry 180 nm beads exposure to oxygen in gaseous phase and as aqueous dispersion (10 mg/mL, T = 25 °C). (d) Photographic images obtained with an RGB camera upon illumination of the planar optical sensor with 366 nm line of a UV-lamp. Bright green phosphorescence indicates the areas of the sensor soaked with an anoxic aqueous solution (containing 5% wt. of glucose and 0.05 % wt. of glucose oxidase) for the left image and the area of the sensor deoxygenated with a flow of nitrogen (below image). (e) Corrected luminescence spectra for the planar optode (λ_{exc} = 365 nm). Inset shows the corresponding Stern-Volmer plots (λ_{max} = 519 nm). (f) Stern-Volmer plots for the sensor based on 320 nm beads dispersed in hydrogel D4 in the gas phase and in water. Response of the dry particles in the gas phase is also shown for comparison. In all the cases T = 25 °C.

The oxygen-sensing properties of the resulting nanoparticles were quantitatively analyzed in gaseous phase first via a phase-modulation technique. Generally, the frequency domain method allows for a compact and inexpensive instrumentation which is important for practical applications.[30] We used 375 nm LED for excitation that almost perfectly matches the absorption maximum of the nanoparticles. Investigation of the dry bead agglomerates revealed a very similar behaviour for 320 and 180 nm NPs (see Figure 3b and Figure S4). As expected, both nanoparticles showed very high oxygen sensitivity which is well explained by the long phosphorescence decay time of the metal-free organic phosphor under oxygen-free conditions ($\tau_{0,gas} \approx 4$ ms, see Figure S4). It should be mentioned that whereas a great amount of oxygen indicators with the phosphorescence decay times from 1 to 1000 µs are available[5,6a] there are only very few examples of probes featuring longer phosphorescence/TADF lifetimes, τ, such as C_{70} fullerene ($\tau_0 \sim 20$ ms),[9b] BF_2-chelates ($\tau_0 \sim 4.3$ ms;[11b] $\tau_0 \sim$ 360-730 ms)[9a] and Gd(III) complexes ($\tau_0 \sim 1.3$ ms; $\tau_0 \sim 2$ ms)[6e] which are of particular interest for design of ultra-sensitive oxygen sensors. The sensitivity is slightly higher for the 320 nm NPs, which is explained by their longer decay time. To quantify the sensitivity, we measured τ as a function of oxygen pressure, pO_2, and plotting τ_0/τ as function of pO_2. The Stern-Volmer plots show a nonlinear behavior, indicating a heterogeneous environment of the quenching sites in the nanoparticles (see Figure 3c). The Stern-Volmer constants, $k_{q1,2}$, were thus evaluated by the 2-site model developed by Carraway and Demas;[31] giving 7.1 kPa^{-1} and 0.28 kPa^{-1} for the first and the second site of the 320 nm NPs, respectively; the LOD in gas phase was estimated to be 5 Pa. Even though linear stern-Volmer plot is advantageous, only very few polymer-immobilized indicators show lineality[32] and good fitting with the 2-site model is fully sufficient for practical application. The resulting high sensitivity makes our nanoparticle system promising for a wide range of industrial and environmental applications, for instance for investigation of oxygen in the oxygen minimum zones in ocean.[33]

The nanoparticles showed some decrease in the luminescence decay time at higher temperatures (see Figure 3b and Figure S4) which is caused by thermal quenching, i.e. increase of non-radiative rate constant. The temperature coefficients are similar for both NPs and are 0.84%/K and 0.72%/K at 25 °C for 320 and

180 nm NPs, respectively; this is higher than those of the most common organometallic oxygen indicators such as Pt(II) and Pd(II) porphyrins and Ru(II) polypyridyl complexes.[34]
Interestingly, nanoparticles dispersed in water showed more linear Stern-Volmer plots and higher sensitivity compared to those in the gas phase, despite slightly shorter decay time (see Figure 3c). The effect of humidity on the sensitivity of oxygen sensors is not uncommon for less hydrophobic polymers.[35] Therefore, the nanoparticle systems introduced here are excellently suitable as well for monitoring of DO in aqueous media. The nanoparticles can be simply added to the analyte solution (e.g. in concentrations of 10 mg/mL) providing that the sample volume is not too large.
In order to achieve higher flexibility in possible applications of the developed material system we prepared planar optodes by dispersing the 320 nm NPs in a polyurethane hydrogel D4. The "cocktail" was coated onto a transparent poly(ethylene terephthalate) (PET) substrate resulting in a thin film (about 14 µm thick) after solvent evaporation. The optodes can be used for imaging[36] of 2D oxygen distributions (illustrated by Figure 3d) or as sensor spots attached to a tip of an optical fiber or placed on the inner side of a transparent glass wall. Red-green-blue (RGB) imaging gained popularity for a variety of practical applications due to its simple and low cost instrumentation.[37] Our nanoparticle system is highly promising for this purpose because the phosphorescence color (λ_{max} at 519 nm) matches almost perfectly the green channel of the camera (see Figure 3e). Although the blue fluorescence at ~ 390nm originating from PET support is not affected by oxygen and, in principle, can be used for referencing of phosphorescence intensity, such measurement is not desirable due to interferences and large scattering effects. For that reason, a reference material which emits in the red part of the spectrum could be added to the sensor layer along with the oxygen-sensitive particles to enable ratiometric read-out. Such ratiometric system is currently under development in our labs. The Stern-Volmer plots for the planar optodes are more linear compared to that of the dry nanoparticle agglomerates (see Figure 3f). The results obtained from the steady state emission spectra (see Figure 3e, inset) and from intensity measurements in frequency domain are very similar (see Figure 3f). Again, the sensitivity is somewhat higher when the measurements are performed in water compared to those with the dry optode, i.e. in the gas phase.[38]
In summary, we have developed metal-free organic phosphors crosslinked within core-shell polymer nanoparticles as a novel versatile platform for highly sensitive detection of DO in a variety of water environments and gaseous oxygen. We believe that this new detection platform will be widely utilized for the convenient and easy monitoring of DO.

Experimental Section

All experimental details are described in supporting information.

Acknowledgements ((optional))

This work was financially supported by National Science Foundation (DMREF DMR 143965). The work in Ulsan was supported by the 2016 Research Fund (1.160022.01) of the Ulsan National Institue of Science and Technology (UNIST) and by the Basic Science Research Program through the National Research Foundation of Korea (NRF), which was funded by the Ministry of Education (NRF-2016R1D1A1B03936002). The work at IMDEA was supported by the Spanish Ministerio de Economía y Competitividad (grant no. CTQ2014-58801).

Keywords: Room temperature phosphorescence (RTP) • Metal-free organic phosphors • Crosslinking • Dissolved oxygen (DO) detection • Polymer nanoparticles

[1] K. Tanno, *Bull. Chem. Soc. Jpn.* **1964**, 37, 804−810
[2] T. Nakano, K. Hoshi, S. Baba, *Vacuum* **2008**, 83, 467−469
[3] H. Berger, *Microelectron. Eng.* **1991**, 10, 259−267
[4] a) D. A. Stolper, N. P. Revsbech, D. E. Canfield, *Proc. Natl. Acad. Sci. USA* **2010**, 107, 18755−18760; b) D. Shevela, K. Beckmann, J. Clausen, W. Junge, J. Messinger, *Proc. Natl. Acad. Sci. USA* **2011**, 108, 3602−3607
[5] X. Wang, O. S. Wolfbeis Chemical Society Reviews, **2014**, 43, 3666-3761.
[6] a) M. Quaranta, S. M. Borisov, I. Klimant, *Bioanal. Rev.* **2012**, 4, 115−157; b) R. Brinas, T. Troxler, R. M. Hochstrasser, S. A. Vinogradov, *J. Am. Chem. Soc*. **2005**, 127, 11851−11862; c) J. A. Spencer, F. Ferraro, E. Roussakis, A. Klein, J. Wu, J. M. Runnels, W. Zaher, L. J. Mortensen, C. Alt, R. Turcotte, R. Yusuf, D. Cote, S. A. Vinogradov, D. T. Scadden, C. P. Lin, *Nature*, **2014**, 508, 269−273; d) Y. Feng, J. Cheng, L. Zhou, X. Zhou, H. Xiang, *Analyst* **2012**, 137, 4885−4901; e) S. M. Borisov, R. Fischer, R. Saf, I. Klimant, Adv. Funct. Mater. 2014, 24, 6548−6560
[7] For recent reviews on metal-free organic phosphors, see: a) S. Mukherjee, P. Thilagar, *Chem. Commun.* **2015**, 51, 109988−11003; b) S. Xu, R. Chen, C. Zheng, W. Huang, *Adv. Mater.* **2016**, 28, 9920−9940; c) M. Baroncini, G. Bergamini, P. Ceroni, *Chem. Commun.* **2017**, 53, 2081−2093; d) S. Hirata, *Adv. Opt. Mater.* **2017**, 1700116
[8] It should be noted that a certain type of RTP emitters having high structural rigidity and small singlet-triplet energy gaps such as benzophenone analogues exhibits rather small Stokes shift.
[9] a) P. Lehner, C. Staudinger, S. M. Borisov, I. Klimant, *Nat. Commun.* **2014**, 5, 4460; b) S. Nagl, C. Baleizão, S. M. Borisov, I. Klimant, *Angew. Chem. Int. Ed.* **2007**, 46, 2317−2319
[10] S. Banerjee, R. T. Kuznetsova, D. B. Pankovsky *Sensors and Actuators B: Chemical* **2015**, 212, 229-234.
[11] a) G. Zhang, J. Chen, S. J. Payn, S. E. Kooi, J. N. Demas, C. L. Fraser. *J. Am. Chem. Soc.* **2007**, 129, 8942−8943; b) G. Zhang, G. M. Palmer, M. W. Dewhirst, C. L. Fraser, *Nat. Mater.* **2009**, 8, 747−751; c) G. Zhang, J. Lu, M. Sabat, C. L. Fraser, *J. Am. Chem. Soc.* **2010**, 132, 2160−2162
[12] a) O. Bolton, K. Lee, H. J. Kim, K. Y. Lin, J. Kim, *Nat. Chem.* **2011**, 3, 205−210; b) D. Lee, O. Bolton, B. C. Kim, J. H. Youk, S. Takayama, J. Kim, *J. Am. Chem. Soc.* **2013**, 135, 6325−6329; c) M. S. Kwon, D. Lee, S. Seo, J. Jung, J. Kim, *Angew. Chem. Int. Ed.* **2014**, 53, 11177−11181; d) M. S. Kwon, Y. Yu, C. Coburn, A. W. Phillips, K. Chung, A. Shanker, J. Jung, G. Kim, K. Pipe, S. R. Forrest, J. H. Youk, J. Gierschner, J. Kim, *Nat. Commun.* **2015**, 6, 8947; e) O. Bolton, D. Lee, J. Jung, J. Kim *Chem. Mater.* **2014**, 26, 6644-6649.
[13] a) W. Z. Yuan, X. Y. Shen, H. Zhao, J. W. Y. Lam, L. Tang, P. Lu, C. Wang, Y. Liu, Z. Wang, Q. Zheng, J. Z. Sun, Y. Ma, B. Z. Tang, *J. Phys. Chem. C* **2010**, 114, 6090−6099; b) Y. Gong, G. Chen, Q. Peng, W. Z. Yuan, Y. Xie, S. Li, Y. Zhang, B. Z. Tang, *Adv. Mater.* **2015**, 27, 6195−6201

[14] M. Koch, K. Perumal, O. Blacque, J. A. Garg, R. Saiganesh, S. Kabilan, K. K. Balasubramanian, K. Venkatesan, *Angew. Chem. Int. Ed.* **2014**, 53, 6378−6382

[15] A. Fermi, G. Bergamini, M. Roy, M. Gingras, P. Ceroni, *J. Am. Chem. Soc.* **2014**, 136, 6395−6400

[16] Y. Xie, Y. Ge, Q. Peng, C. Li, Q. Li, Z. Li, *Adv. Mater.* **2017**, 29, 1606829

[17] Z. Yang, Z. Mao, X. Zhang, D. Ou, Y. Mu, Y. Zhang, C. Zhao, S. Liu, Z. Chi, J. Xu, Y. Wu, P. Lu, A. Lien, M. R. Bryce, *Angew. Chem. Int. Ed.* **2016**, 55, 2181−2185

[18] J. Xu, A. Takai, Y. Kobayashi, M. Takeuchi, *Chem. Commun*. **2013**, 49, 8447−8449

[19] a) S. Hirata, K. Totani, J. Zhang, T. Yamashita, H. Kaji, S. R. Marder, T. Watanabe, C. Adachi, *Adv. Funct. Mater.* **2013**, 23, 3386−3397; b) R. Kabe, N. Notsuka, K. Yoshida, C. Adachi, *Adv. Mater.* **2016**, 28, 655−660

[20] a) Z. An, C. Zheng, Y. Tao, R. Chen, H. Shi, T. Chen, Z. Wang, H. Li, R. Deng, X. Liu, W. Huang, *Nat. Mater.* **2015**, 14, 685−690; b) X. Zhen, Y. Tao, Z. An, P. Chen, C. Xu, R. Chen, W. Huang, K. Pu, *Adv. Mater.* **2017**, 1606665; c) S. Cai, H. Shi, J. Li, L. Gu, Y. Ni, Z. Cheng, S. Wang, W. Xiong, L. Li, Z. An, W. Huang, *Adv. Mater*. **2017**, 1701244

[21] Y. Shoji, Y. Ikabata, Q. Wang, D. Nemoto, A. Sakamoto, N. Tanaka, J. Seino, H. Nakai, T. Fukushima, *J. Am. Chem. Soc.* **2017**, 139, 2728−2733

[22] X. Chen, C. Xu, T. Wang, C. Zhou, J. Du, Z. Wang, H. Xu, T. Xie, G. Bi, J. Jiang, X. Zhang, J. N. Demas, C. O. Trindle, Y. Luo, G. Zhang, *Angew. Chem. Int. Ed.* **2016**, 55, 9872−9876

[23] Z. Mao, Z. Yang, Y. Mu, Y. Zhang, Y. Wang, Z. Chi, C. Lo, S. Liu, A. Lien, J. Xu, *Angew. Chem. Int. Ed.* **2015**, 54, 6270−6273

[24] D. Chaudhuri, E. Sigmund, A. Meyer, L. Rock, P. Klemm, S. Lautenschlager, A. Schmid, S. R. Yost, T. V. Voorhis, S. Bange, S. Hoger, J. M. Lupton, *Angew. Chem. Int. Ed.* **2013**, 52, 13449−13452

[25] S. Reineke, M. A. Baldo, *Sci. Rep*. **2014**, 4, 3797

[26] R. A. Petros, J. M. DeSimone, *Nat. Rev. Drug. Discov.* **2010**, 9, 615−627

[27] Y. C. Yu, H. S. Cho, W. Yu, J. H. Youk, *Polymer* **2014**, 55, 5986−5990

[28] X. Zhang, S. Boisse, W. Zhang, P. Beaunier, F. D'Agosto, J. Rieger, B. Charleux, *Macromolecules* **2011**, 44, 4149−4158

[29] Without incorporation of the PAAm block, RAFT polymerization of styrene was not successful because of a few possible problems such as low conversion, homopolymer formation, and broad size distribution of nanoparticles.

[30] O. S. Wolfbeis, BioEssays, **2015**, 37, 921−928

[31] E. R. Carraway, J. N. Demas, B. A. DeGraff, J. R. Bacon, *Anal. Chem.* **1991**, 63, 337−342

[32] S. M. Borisov, P. Lehner, I. Klimant, Anal. Chim. Acta. 2011, 690, 108−115

[33] N. Revsbech, L. H. Larsen, J. Gundersen, T. Dalsgaard, O. Ulloa, *Limnol. Oceanogr. Methods,* **2009**, 7, 371−381

[34] S. M. Borisov, I. Klimant, *Anal. Chem.* **2007**, 79, 7501−7509

[35] K. Eaton, P, Douglas, Sens. Actuators, B. 2002, 82, 94−104

[36] M. Schaferling, *Angew. Chem. Int. Ed.* **2012**, 51, 3532−3554

[37] a) M. Larsen, S. M. Borisov, B. Grunwald, I. Klimant, R. N. Guld, *Limnol. Oceanogr. Methods,* **2011**, 9, 348−360; b) X. Wang, R. J. Meier, M. Link, O. S. Wolfbeis, *Angew. Chem. Int. Ed.* **2010**, 49, 4907−4909; c) R. J. Meier, L. H. Fischer, O. S. Wolfbeis, M. Schaferling, *Sens. Actuators, B* **2013**, 177, 500−506

[38] Photostability of our optical sensor system was discussed in detail in the SI.

COMMUNICATION

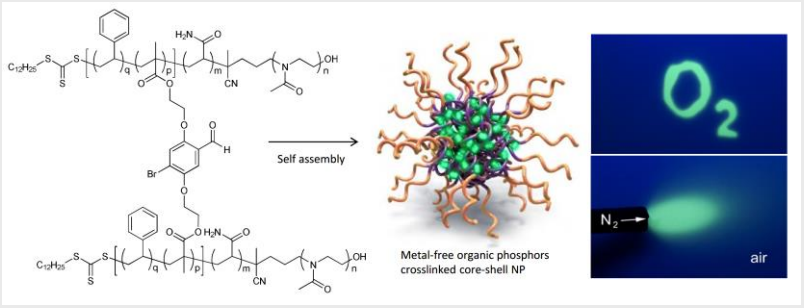

We report a highly sensitive dissolved oxygen (DO) detection platform based on core-shell nanoparticles with water-soluble polymethyloxazoline shell and oxygen-permeable polystyrene core crosslinked with metal-free purely organic phosphors. The resulting nanoparticles show a very high sensitivity (LOD of 60nM DO) and can be readily used for oxygen quantification in a variety of environments.

*Y. Yu,[†] M. S. Kwon,[†,]*J. Jung, Y. Zheng, M. Kim, K. Chung, J. Gierschner, J. H. Youk,* S. M. Borisov,* J. Kim**

Page No. – Page No.

Room Temperature Phosphorescence based Dissolved Oxygen Detection by Metal-free Organic Phosphor Containing Core-shell Polymer Nanoparticles